Technical Report

# Adjoint Flow Solver `TinyFlow` using `dco/c++`

**Johannes Lotz[1]* and Viktor Mosenkis[2]**

1 Software and Tools for Computational Engineering

2 Numerical Algorithms Group

**Abstract:** Adjoints of large numerical solvers are used more and in industry and academia, e.g. in computational fluid dynamics, finance and engineering. Using algorithmic differentiation is a convenient and efficient of generating adjoint codes automatically from a given primal. This document reports the application of algorithmic differentiation using `dco/c++` to a demonstrator flow solver, which makes use of various NAG Library routines. Since the NAG Library supports `dco/c++` data types, seamless integration is possible (as shown in this report). Simple switches between algorithmic and symbolic versions of the NAG routines can be used to minimize memory usage.

**Keywords:** NAG Library ● Adjoints ● Algorithmic Differentiation ● `dco/c++` ● CFD

## 1. Introduction

This technical report serves as a demonstrator on how to use `dco/c++` and the NAG AD Library to compute adjoints of a non-trivial PDE (partial differential equation) solver. It shows how `dco/c++` can be used to couple hand-written symbolic adjoint code with an overall algorithmic solution; but it also demonstrates the easy-to-use interface when `dco/c++` is coupled with the NAG AD Library (`nag.co.uk/content/adjoint-algorithmic-differentiation` – referred to as *webpage* in the following). Here, the sparse linear solver `f11jc` can be switched from algorithmic to symbolic mode in one code line.

The next section introduces the primal solver followed by sections about the adjoint solver and respective run time and memory results. Also, an optimization algorithm is run on a test case using steepest descent to show potential use of the computed adjoints.

## 2. Primal Solver

`TinyFlow` is a non-validated three-dimensional unsteady incompressible DNS (direct numerical simulation, i.e. no turbulence model) solver with Boussinesq approximation [1, 2] for modeling temperature dependency on vertical

* *E-mail: lotz@stce.rwth-aachen.de*

forces. The respectively simplified Navier–Stokes equations are solved on an equidistant Cartesian grid with finite difference discretization. The code was originally written by J. Lotz while working at the Institute of Meteorology and Climatology (MuK), University of Hanover in 2010. The implementation was first written in Fortran and later translated into C++. The Fortran implementation was based on the numerics used in the simulation software PALM [3], developed at the MuK, which is a production sized parallelized simulation code for atmospheric boundary layers. In addition, `TinyFlow` features a porosity term which can be used for topology optimization [4, 14]. Over time, `dco/c++` and `dco/fortran` (see *webpage*) were employed on `TinyFlow` for research as well as teaching activities.

`TinyFlow` is a fully templated code with ∼1800 lines-of-code. It uses a configuration file for physical and numerical parameters and stores results in the VTK file format (`vtk.org`) which can then be read and visualized, e.g., using paraview (`paraview.org`).

## 2.1. Governing Equations

The Boussinesq approximation simplifies the Navier–Stokes equation by assuming incompressibility, but taking into account the forces generated by (small) temperature variations. The momentum equation for the state variables $\mathbf{u} \in I\!R^3$ (the three velocity components into $x$-, $y$-, and $z$-direction) takes the form

$$\frac{\mathrm{d}\mathbf{u}}{\mathrm{d}t} = -\left(\mathbf{u}\cdot\nabla\right)\mathbf{u} + \nu\nabla^2\mathbf{u} - \frac{1}{\rho}\nabla p - g\frac{T-T_0}{T_0}\mathbf{e}_3 + \alpha\mathbf{u} \tag{1}$$

where $\nu$ the dynamic viscosity, $\rho$ the density, $p$ the pressure, and $T/T_0$ the temperature/reference temperature. $g$ is the gravity constant and $\mathbf{e}_3$ the third Cartesian basis vector. $\alpha \in I\!R$ is a scalar porosity coefficient; the smaller $\alpha$ (i.e. negative) is at some point in space, the more drag will be enforced upon the flow.

In addition, mass conservation is ensured by the usual incompressibility equation

$$\nabla\cdot\mathbf{u} = \nabla^2 p\,. \tag{2}$$

## 2.2. Numerical Methods

Equations (1) and (2) are discretized using finite difference schemes on an equidistant Cartesian grid, which is of attractive simplicity. The state variables are defined on a staggered Arakawa-C grid, see Figure 1. Equations (1) and (2) are solved decoupled by a predictor-corrector method, i.e.

1. the momentum equation (1) is solved with a given pressure for the velocities and temperature at the new time step, and
2. corrected afterwards using the Poisson equation (2).

The time is discretized using the implicite or explicit Euler method (both schemes implemented), while the space is descretized with central finite difference for the second-order terms, and using the Piascek-Williams [9] scheme for the first-order terms.

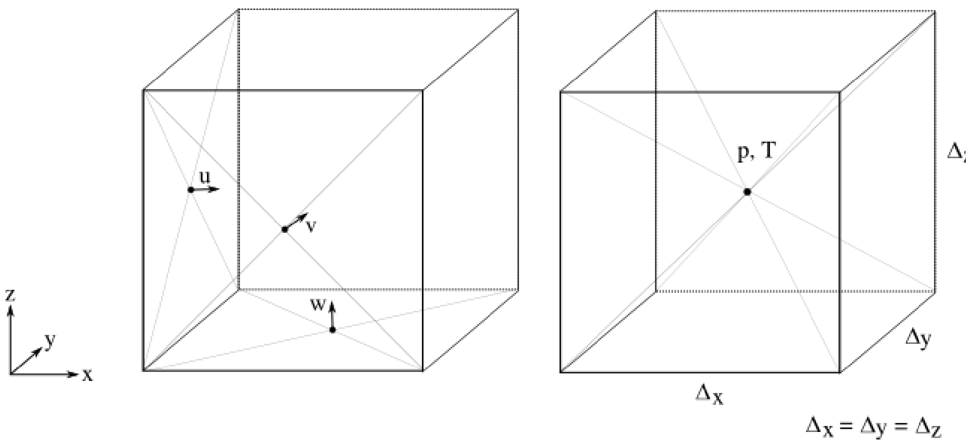

Figure 1: Visualization of Arakawa-C grid: velocities are defined on faces (x-velocity $u$, y-velocity $v$, z-velocity $w$), pressure $p$ and temperature $T$ at cell centers.

For backward (i.e. implicit) Euler, the momentum equation yields a nonlinear residual function $F = F(\mathbf{v}^{i+1}, \mathbf{v}^i, \boldsymbol{\alpha})$, $F : I\!R^{n+n+n} \rightarrow I\!R^n$ per iteration with state $\mathbf{v}^{i+1} \in I\!R^n$ at the next time step, state $\mathbf{v}^i \in I\!R^n$ at the current time step, and parameter $\boldsymbol{\alpha} \in I\!R^n$. $n$ is the degree of freedom in the state variable $\mathbf{v}^i$ representing the three-dimensional velocity field as well as the temperature distribution. $F$ is given as

$$F(\mathbf{v}^{i+1}, \mathbf{v}^i, \boldsymbol{\alpha}) = \mathbf{v}^i - \mathbf{v}^{i+1} + \Delta t f(\mathbf{v}^{i+1}, \boldsymbol{\alpha}) \tag{3}$$

with $f$ being the discretized right-hand side of Equation (1). Applying Newton's algorithm to solve $F(\mathbf{v}^{i+1}, \mathbf{v}^i, \boldsymbol{\alpha}) = 0$, we get the iteration

$$\mathbf{v}^{i+1} = \mathbf{v}^i + \mathbf{x}^i \quad \text{with} \quad \frac{\partial F}{\partial \mathbf{v}^{i+1}} \cdot \mathbf{x}^i = -F\ . \tag{4}$$

In `TinyFlow` the linear system with the Jacobian is solved iteratively and matrix-free with BiCG using the tangent model of AD to compute required Jacobian-vector products

$$\mathbf{y} = \frac{\partial F}{\partial \mathbf{v}^{i+1}} \cdot \mathbf{x} \quad \text{for arbitrary } \mathbf{x}\ . \tag{5}$$

The linear system is preconditioned using Jacobi-preconditioning.

For explicit Euler, $F$ can be used to get the time iteration

$$\begin{aligned} \mathbf{v}^{i+1} &= \mathbf{v}^i + F(\mathbf{v}^i, \mathbf{v}^i, \boldsymbol{\alpha}) \\ &= \mathbf{v}^i + \mathbf{v}^i - \mathbf{v}^i + \Delta t f(\mathbf{v}^i) \\ &= \mathbf{v}^i + \Delta t f(\mathbf{v}^i)\ . \end{aligned} \tag{6}$$

## 2.3. Test Case

The test case is chosen to be a cube with a 1m side length. Velocity has no-slip boundary conditions and temperature has everywhere Dirichlet boundary conditions. At two spots at the bottom, the temperature is set to a value 30K warmer than everywhere else. Initial conditions are chosen to be zero for all velocities and constant to 273K for the temperature. See Figure 2 for a visualization. The flow solution after six seconds is shown in

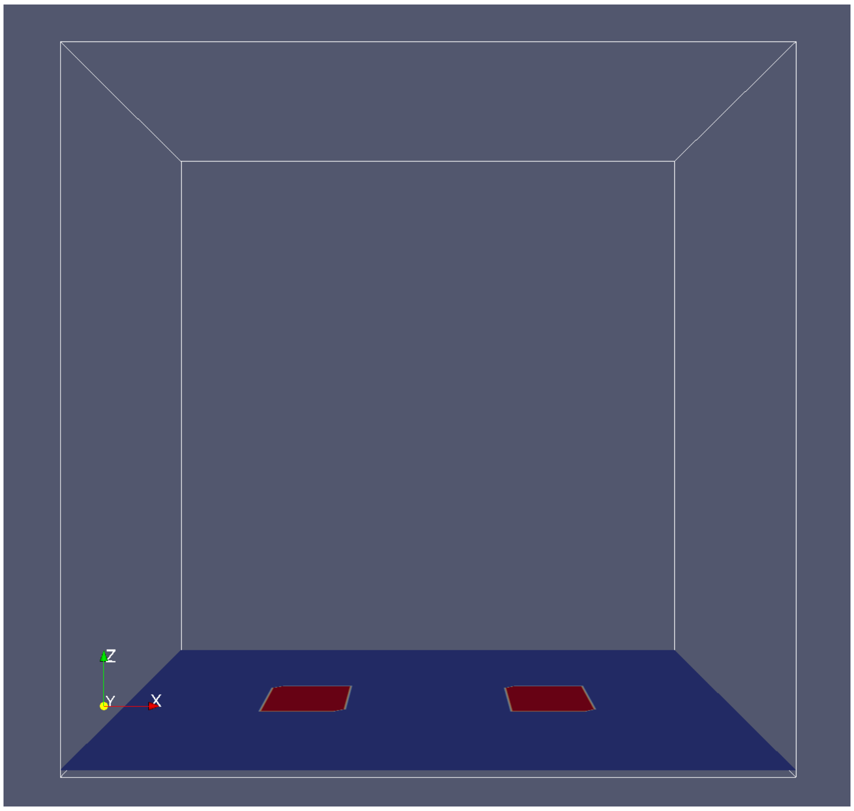

Figure 2: Visualization of the test case. At the bottom, the color shows the temperature distribution (red: warmer). $z$ is the vertical axis, $x$ and $y$ the horizontal.

Figure 3a. Putting a plate in the middle of the cube using the $\boldsymbol{\alpha}$ term in Equation (1) results in a flow solution shown in Figure 3b.

## 2.4. Implementation

The code is writte in C++ using selected features from C++14. It is fully templated and is build upon NAG Library routines for the numerical core, i.e. solving the linear systems with sparse or matrix-free methods. The following NAG routines are used:

- `f11ja`: computes an incomplete Cholesky factorization of a real sparse symmetric matrix, represented in

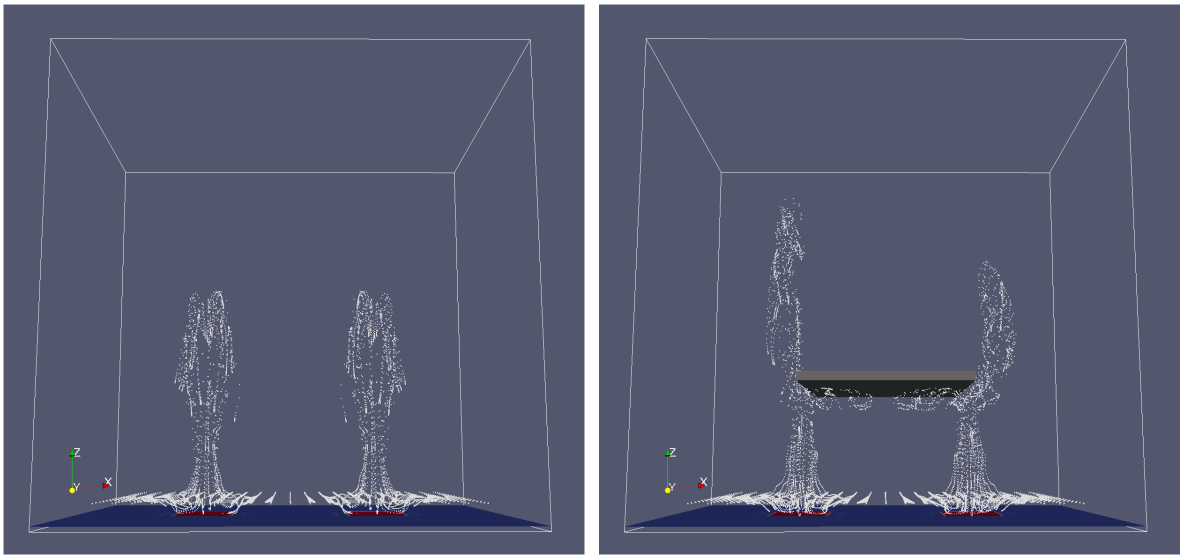
(a) Without plate. (b) With plate. Plate is sligthly shifted to the left, i.e. not a symmetric flow.

Figure 3: Flow solutions of the test case with and without a plate in the middle of a 1m side length cube with two heat sources at the bottom.

symmetric coordinate storage format. This factorization is used as a preconditioner in combination with `f11jc`.

- `f11jc`: solves a real sparse symmetric system of linear equations, represented in symmetric coordinate storage format, using a conjugate gradient or Lanczos method, with incomplete Cholesky preconditioning.
- `f11be`: an iterative solver for a real general (nonsymmetric) system of simultaneous linear equations.
- `f11bd`: the setup routine for the iterative solution of a real general (nonsymmetric) system of simultaneous linear equations with `f11be`.

A documented example of the main program is given in the following. As can be seen, all used classes are templated, such that a type change can easily be achieved later for computing tangents or adjoints with `dco/c++`.

```cpp
#include "TinyFlow.hpp"
int main(int argc, char **argv) {
  //** reads numerical parameters from file
  parameters_t p(argv[1]);

  //** allocates and holds all state variables
  variables_t<double> v(p);

  //** defines equation/residual and numerical methods
  equation_t<double> e(p);

  //** defines the objective
  cost_functional_t<double> J(p);

  //** run time integrator (static function)
  integrator_t<double>::run(p, e, v, J);

  cout << "objective = " << J.get() << endl;
  return 0;
}
```

Printing the parameters `p` to `std::cout` might result in

```
PARAMETERS:
===========
 physical:
      g_earth = 9.81
      nu = 1.7e-05
      kappa = 2.62e-05
      rho = 1.204
      t0 = 293
      t_end = 5
      nx = 10
      ny = 10
      nz = 10
 numerical:
      pressure_solver = 1
      timestepping = 1
      pressure_solver_eps = 0.01
      newton_eps = 0.01
      pressure_solver_max_iter = 5000
      opti_max_iter = 5
      omega = 1.4
      max CFL = 0.1
      dt = 0.01
 various:
      save_to_file_dt = 0.1
      text_output = 2
```

### 2.4.1. Momentum Equation

As described in Section 2.2, the momentum is either solved with explicit or implicit Euler. For the explicit case, no further comments are required. The implicit solver needs to solve the nonlinear system

$$F(\mathbf{v}^{i+1}, \mathbf{v}^{i}, \boldsymbol{\alpha}) = \mathbf{v}^{i} - \mathbf{v}^{i+1} + \Delta t f(\mathbf{v}^{i+1}) = 0 \tag{7}$$

with $f$ being the discretized right-hand side of Equation (1) for unknown state $\mathbf{v}^{i+1}$, given state $\mathbf{v}^{i}$, and parameters $\boldsymbol{\alpha}$. $F$ is implemented as a templated residual function with the following specification:

```
template <typename U, typename RES_P>
std::vector<U> residual(parameters_t const& flow_parameters,
                        std::vector<U> const& V,
                        RES_P const& res_parameters)
```

where `flow_parameters` hold the necessary constants (e.g. gravity constant) as well as numerical parameters (e.g. timestep $\Delta t$), `V` holds $\mathbf{v}^{i+1}$, and `res_parameters` holds $\mathbf{v}^{i}$ as well as $\boldsymbol{\alpha}$. The returned value is the residual. This residual function can now easily be used in the iterative BiCG solver `f11be` as shown in the next code listings. It is now assumed that you are familiar with the used NAG routines as well as `dco/c++` usage. The code in `case 1` needs to compute the Jacobian-vector product from Equation (5).

```
F11BEF(irevcm, x, y, wgt, work, lwork, fail);
while (irevcm != 4) {
  switch (irevcm) {
  case 1:
    //** compute Jacobian-vector product
    // set tangent of v^{i+1} to x
    dco::derivative(v) = x;
    // get tangent of F and store to y
    y = dco::derivative(residual(flow_p, v, res_p));
    break;
  case 2:
    //** preconditioner
  };
  F11BEF(irevcm, x, y, wgt, work, lwork, fail);
}
```

This linear system solver is embedded into a standard Newton algorithm.

### 2.4.2. Pressure Solver

The pressure solver needs to solve symmetric sparse systems using `f11jc`. The system matrix is constant over all time steps, and therefore the incomplete Cholesky factorization which is used as the preconditioner needs to be computed only once using `f11ja`. An alternative method using SOR (Successive Over-Relaxation) is also implemented.

# 3. Adjoint Solver

The overall adjoint is computed using dco/c++ with the following driver. Only differences to the listing in Section 2.4 are documented.

```cpp
#include "dco.hpp"
#include "TinyFlow.hpp"

//** define mode and type of dco/c++ to be used: adjoint
using adjoint_m = dco::ga1s<double>;
using adjoint_t = adjoint_m::type;

int main(int argc, char **argv) {
  //** allocate global tape / data structure for reversal
  adjoint_m::global_tape = adjoint_m::tape_t::create();

  parameters_t p(argv[1]);

  //** instantiate all classes with dco/c++ type
  variables_t<adjoint_t> v(p);
  equation_t<adjoint_t> e(p);
  cost_functional_t<adjoint_t> cost_functional(p);

  //** register parameters we want to have the gradient w.r.t; here: \alpha
  adjoint_m::global_tape->register_variable(v.alpha());

  integrator_t<adjoint_t>::run(p, e, v, cost_functional);

  //** set output adjoint to 1.0
  dco::derivative(cost_functional.get()) = 1.0;

  //** propagate adjoints through tape (reversal)
  adjoint_m::global_tape->interpret_adjoint();

  //** get gradient of J w.r.t. alpha
  for (auto& a : v.alpha())
    std::cout << dco::derivative(a) << std::endl;

  //** free memory
  adjoint_m::tape_t::remove(adjoint_m::global_tape);
  return 0;
}
```

Since TinyFlow is an unsteady solver, common approaches for steady flow solvers like reverse accumulation [13] or piggyback [12] cannot be used.

As described in [10], dco/c++ can be coupled with hand-written or externally differentiated adjoint solutions. In addition, NAG routines can seamlessly be integrated into the dco/c++ solution via the NAG AD Library, as described on the *webpage*. Since a fully algorithmic treatment requires a huge amount of memory, the NAG AD

Library provides robust (i.e. symbolic and checkpointed) versions of some routines, including `d02cj` [11] and the used `f11jc`.

In `TinyFlow` both techniques are used. For the implicit solution of the momentum equation, a hand-written adjoint is implemented exploiting the implicit function theorem [10]. For the pressure solver, NAG's symbolic adjoint implementation is used.

## 3.1. Momentum Equation

Symbolic treatment of the nonlinear solver as shown in [10] for an overall adjoint requires per reverse time step the solution of a linear system of type

$$\left(\frac{\partial F}{\partial \mathbf{v}^{i+1}}\right)^T \cdot \mathbf{b} = \bar{\mathbf{v}}^{i+1} \ , \quad \mathbf{v}^{i+1}, \bar{\mathbf{v}}^{i+1}, \mathbf{b} \in I\!R^n \tag{8}$$

with incoming adjoints $\bar{\mathbf{v}}^{i+1}$. This is followed by one adjoint propagation

$$\begin{pmatrix} \bar{\mathbf{v}}^i \\ \bar{\boldsymbol{\alpha}} \end{pmatrix} += \left(\frac{\partial F}{\partial(\mathbf{v}^i, \boldsymbol{\alpha})}\right)^T \cdot \mathbf{b} \ . \tag{9}$$

This equation motivates the respective interface of the residual function shown in Section 2.4.1. We need to distinguish between $\mathbf{v}^{i+1}$ on the one hand and $(\mathbf{v}^i, \boldsymbol{\alpha})$ on the other.

The system in Equation (8) can be solved again matrix-free and iteratively with BiCG (alike the primal, see Section 2.2) using the *adjoint* model of $F$ to compute transposed Jacobian-vector products

$$\mathbf{y} = \left(\frac{\partial F}{\partial \mathbf{v}^{i+1}}\right)^T \cdot \mathbf{x} \quad \text{for arbitrary } \mathbf{x} \ . \tag{10}$$

The same Jacobi preconditioner can be used. The respective code section implementing Equation (8) is given as:

```
//** since we're using one global tape, we have to reset to the
//** current position later
auto pos = tape->get_position();

//** register V^{i+1} and record tape; this only needs to be done
//** once, since the same tape can be reinterpreted with different
//** output adjoints, see below in 'case 1'
tape->register_variable(v);
auto res = residual(flow_p, v, cparams);

//** the following computation should not be taped
tape->switch_to_passive();

//** run solver
F11BEF(irevcm, x, y, wgt, work, lwork, fail);
while (irevcm != 4) {
  switch (irevcm) {
  case 1:
    //** compute transposed matrix-vector-product using the tape
    dco::derivative(res) = u;
    tape->interpret_adjoint_to(pos);
    v = dco::derivative(x);
    tape->zero_adjoints_to(pos);
    break;
  case 2:
    //** preconditioner
  };
  F11BEF(irevcm, x, y, wgt, work, lwork, fail);
}
```

The respective code section implementing Equation (9) is given as:

```
//** as described in previous listing, we need to reset state in global tape
tape->reset_to(pos);

//** passivate vi, adjoints w.r.t. parameters only
for (auto& vi : v) vi = dco::value(vi);

//** record
tape->switch_to_active();
res = residual(flow_p, x, params);

//** set output adjoint to solution of adjoint linear system
dco::derivative(res) = b;

//** propagate into parameters (not required to be registered
//** beforehand in this special case) and reset tape to original state
tape->interpret_adjoint_and_reset_to(pos);
```

## 3.2. Pressure Solver

The adjoint of the pressure solver can ignore the incomplete Cholesky factorization needed for preconditioning, since the matrix is constant and has therefore zero derivatives. Only the adjoint of the solution of the linear systems with respect to its right-hand side need to be addressed. The default behaviour when calling NAG routines with dco/c++ types is to compute fully algorithmic adjoint. This usually requires a huge amount of memory. Therefore, symbolic approaches can be used in the following way:

```
void *ad_config = dco::a1w::create_config();
dco::a1w::adjoint_mode(ad_config) = nagad_symbolic;

F11JCF(ad_config, method, _n, _nnz, _a, _la, _irow, _icol, _ipiv, _istr, b,
       tol, maxitn, x, rnorm, itn, work, lwork, fail, method_len);

dco::a1w::remove_config(ad_config);
```

Since the NAG AD Library provides symbolic versions of specific routines, this is just a matter of switching the correct flag in the `ad_config` object.

## 4. Results

In this section, we first look at the gradient computation of the objective

$$J(\boldsymbol{\alpha}) = \sum_i \int_{(x,y,z)\in O_i} w_i u_z(t^{\text{end}}) \; . \tag{11}$$

with respect to the parameter $\boldsymbol{\alpha}$. The objective integrates over subdomains $O_i$ the vertical velocity $u_z$ with a weighting constant $w_i$. We choose two subdomains visualized in Figure 4, where $w_1 = 1$ and $w_2 = -1$. Memory

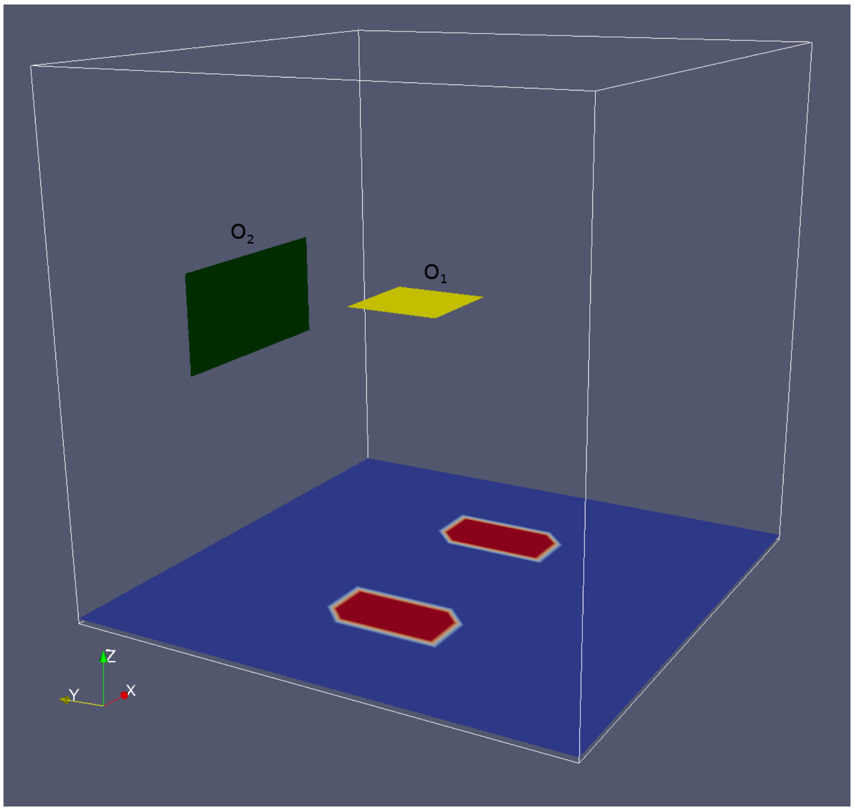

Figure 4: Visualization of the objective. The yellow plate shows the subdomain $O_1$, where the upwards pointing vertical velocity is measured; the green plate shows the subdomain $O_2$, where the downwards pointing velocity is measured.

consumption and run time is shown for the various configurations. Afterwards, results for an optimization using the steepest descent algorithm are shown.

| **Configuration** | **Run Time [s] (Forward)** | **Run Time [s] (Reverse)** | **Memory [MB]** |
|---|---|---|---|
| passive | 0.2 | – | (no additional) |
| finite differences | 1152 | – | (no additional) |
| tangent | 9307 | – | (no additional) |
| adjoint (fully algorithmic) | 5.4 | 1.0 | 6721 |
| adjoint (symbolic f11jc) | 4.1 | 0.9 | 4963 |
| adjoint (symbolic Newton) | 2.3 | 0.6 | 2175 |
| adjoint (fully symbolic) | 1.1 | 0.3 | 84 |

Table 1: Run time and memory consumption for the various configurations. As can be seen, the total ratio of an adjoint evaluation to one primal evaluation comes down to 7 for the fully symbolic case. Memory consumption comes down to 84MB.

## 4.1. Gradient Computation

The following configurations can be compared:

- finite differences of `TinyFlow` using `double`
- tangent version of `TinyFlow` using `dco/c++` tangent types
- adjoint version of `TinyFlow` using `dco/c++` adjoint types
  - algorithmic or symbolic linear solver `f11jc`
  - explicit or implicit Euler timestepping
  - if implicit Euler, algorithmic or symbolic Newton solver

As shown in Figure 5, the numerical values of the gradients computed by adjoint algorithmic differentiation and finite differences coincide quite well for the explicit as well as for the implicit Euler.
When comparing the gradient for the different solutions with implicit and explicit Euler, the values also seem to match quite well, see Figure 6. Tangent and adjoint versions match up to machine precision.

## 4.2. Topology Optimization

Availability of cheap gradient computations allows the running a steepest descent for the given objective Equation (11). The optimized $\boldsymbol{\alpha}^*$ is shown in Figure 7. Respective flow solutions at last timestep are shown in Figure 8.

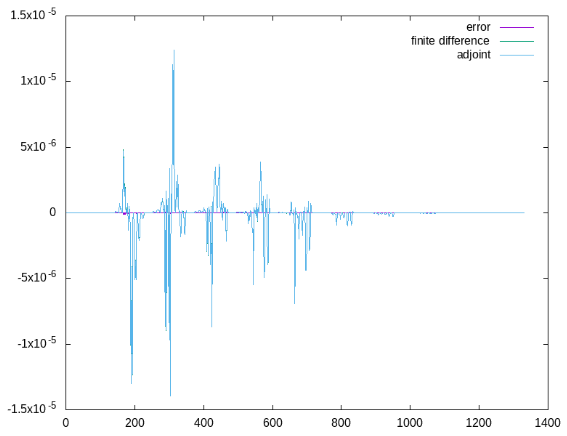

(a) Full Gradient; implicit Euler.

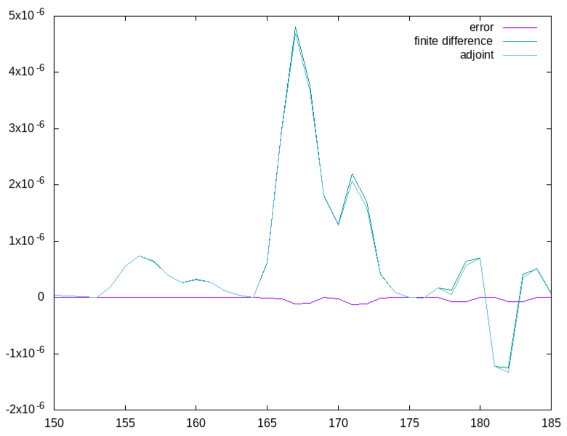

(b) Zoom; implicit Euler.

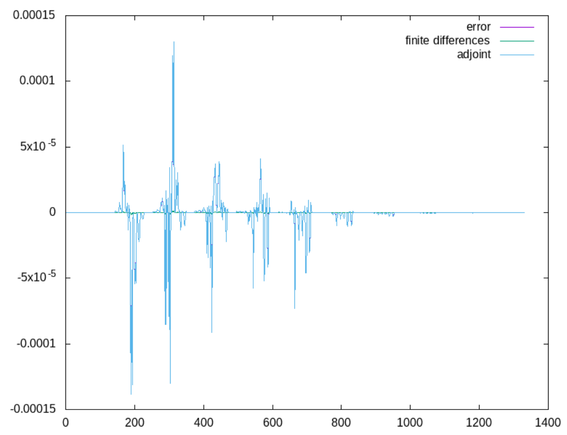

(c) Full Gradient; explicit Euler.

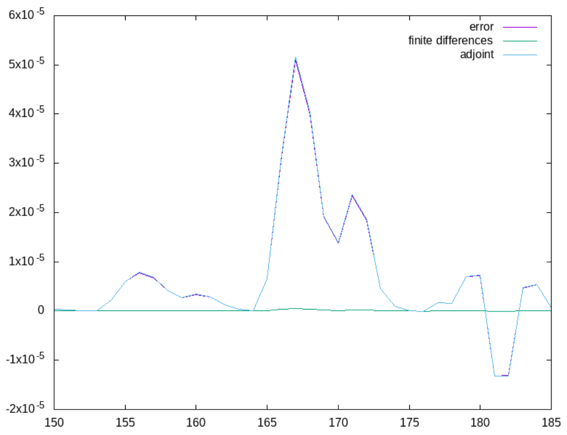

(d) Zoom; explicit Euler.

Figure 5: Implicit Euler with $\Delta t = 0.1$ and explicit Euler with $\Delta t = 0.01$. Both have a resolution of $10 \times 10 \times 10$ grid points. Comparison of gradient computed by finite differences and adjoint AD. The explicit case shows less differences. This might be because of the smaller timestep (which is required for stability).

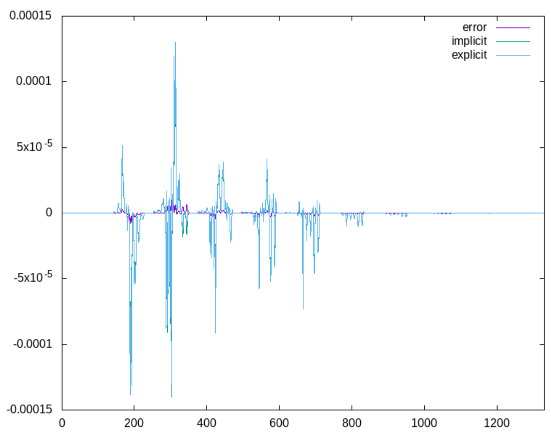

(a) Full Gradient.

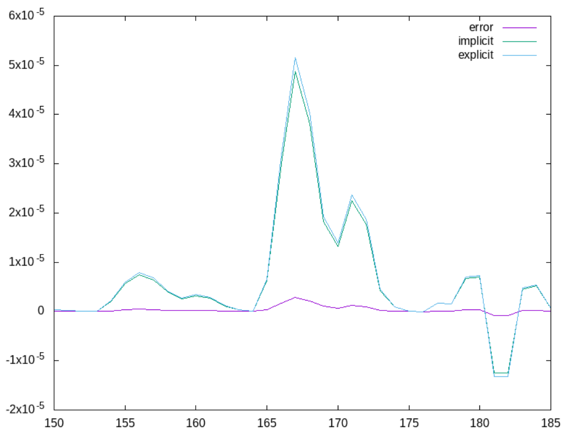

(b) Zoom.

Figure 6: Explicit vs. Implicit Euler with a resolution of $10 \times 10 \times 10$ grid points: Comparison of gradient computed with $\Delta t = 0.01$ in the explicit case and with $\Delta t = 0.1$ for the implicit case.

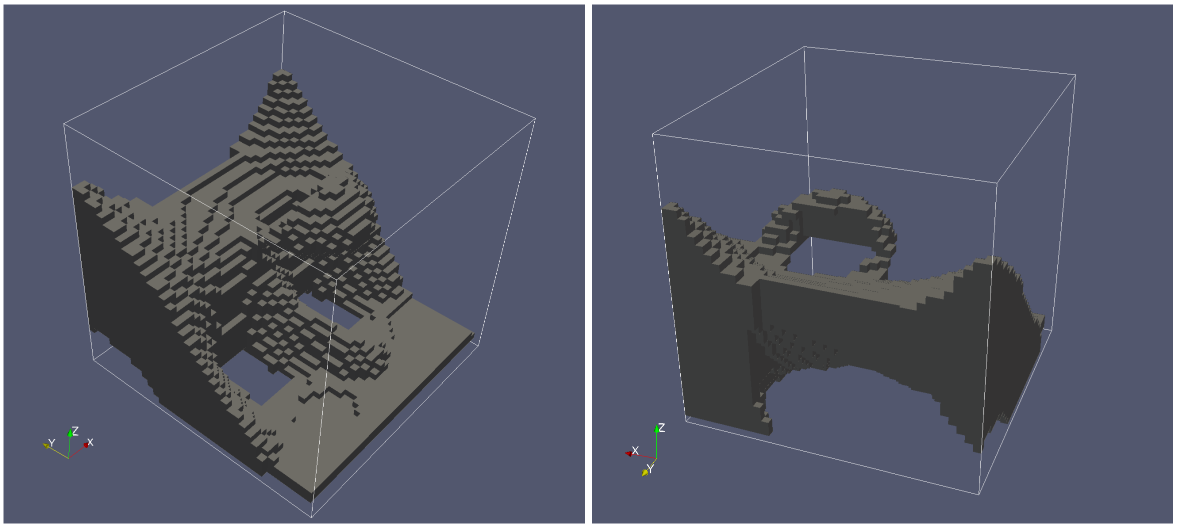

Figure 7: Visualization from two different angles of optimized $\boldsymbol{\alpha}^*$ for objective Equation (11). Both subdomains are left free of any material, while the flow is actually guided by the material to the respective domains.

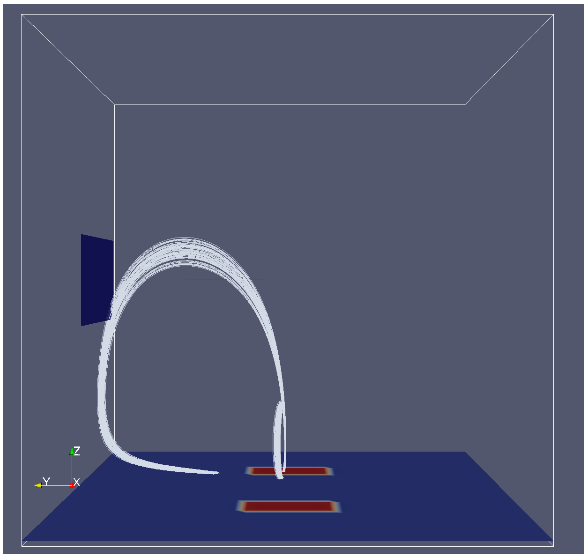

(a) Before Optimization. Streamlines through $O_1$.

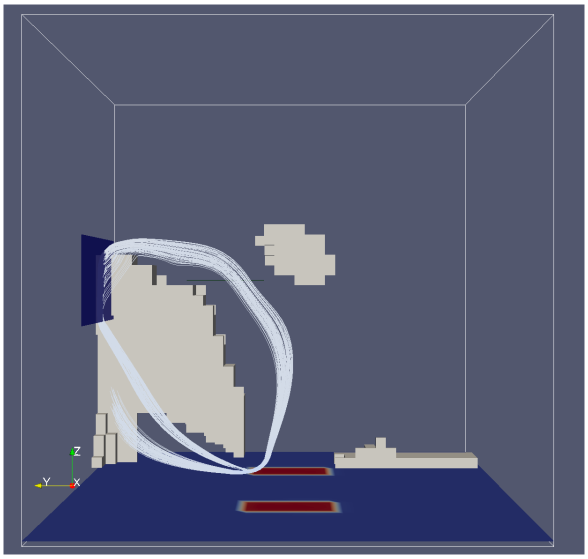

(b) After Optimization. Streamlines through $O_1$. One can see, that the flow has a larger vertical component at $O_1$.

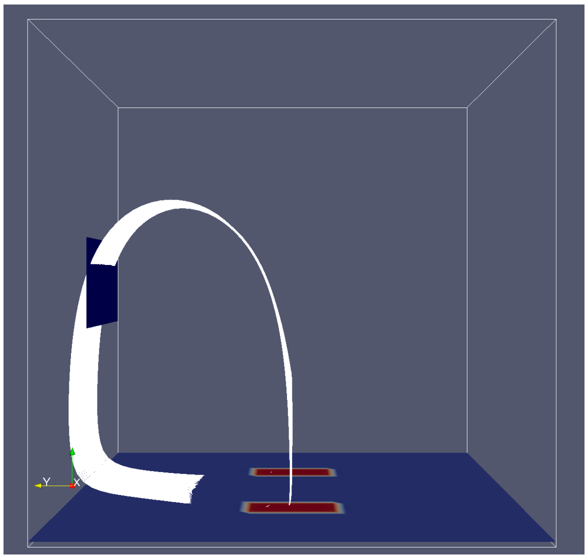

(c) Before Optimization. Streamlines through $O_2$.

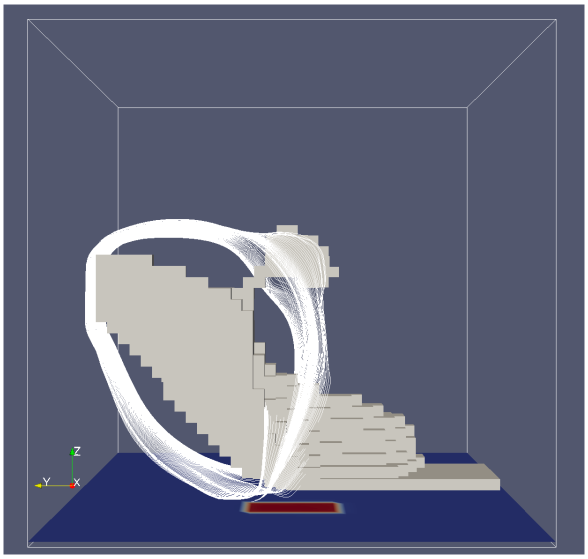

(d) After Optimization. Streamlines through $O_2$. The better match of the vertical component through $O_2$ is obvious.

Figure 8: Visualization of the flow solution at end time, where the objective Equation (11) is defined before and after optimization for two different streamline sets. Material is cut of for visualization purposes only.

## References

[1] D. Etling: Theoretische Meteorologie. Eine Einfhrung. Springer, 2008.

[2] J. Boussinesq: Théorie Analytique de la Chaleur. Gauthier-Villars, 1903.

[3] S. Raasch and M. Schröter: PALM – a Large-Eddy Simulation Model Performing on Massively Parallel Computers. E. Schweizerbart'sche Verlagsbuchhandlung, Meteorologische Zeitschrift, Vol. 10, Nr. 5, 2001.

[4] C. Othmer and E. de Villiers: Implementation of a continuous adjoint for topology optimization of ducted flows. 18th AIAA Computational Fluid Dynamics Conference, 2007.

[5] U. Naumann, J. Lotz, K. Leppkes, M. Towara: Algorithmic Differentiation of Numerical Methods: First-Order Tangents and Adjoints for Solvers of Systems of Nonlinear Equations. ACM ToMS, 41(4):26:1-26:21.

[6] J. Lotz, U. Naumann, R. Hannemann-Tamas, T. Ploch, and A. Mitsos: Higher-Order Discrete Adjoint ODE Solver in C++ for Dynamic Optimization. Procedia Computer Science, 2015 International Conference on Computational Science.

[7] A. Griewank and A. Walther: Evaluating Derivatives, 2nd Edition. SIAM, 2008.

[8] A. Griewank and A. Walther: Algorithm 799: Revolve: An Implementation of Checkpoint for the Reverse or Adjoint Mode of Computational Differentiation Article. ACM ToMS, 2000.

[9] S. Piascek, G. Williams: Conservation properties of convection difference schemes. J. Comput. Phys. 198, 1970.

[10] U. Naumann, J. Lotz, K. Leppkes, and M. Towara: Algorithmic Differentiation of Numerical Methods: Tangent and Adjoint Solvers for Parameterized Systems of Nonlinear Equations, ACM ToMS, 2016.

[11] J. Lotz: Robust Adjoints of the ODE Solver `d02cj`. Internal Technical Report, 2018.

[12] A. Griewank and C. Faure: Piggyback Differentiation and Optimization. Large-Scale PDE-Constrained Optimization, Springer, 2003.

[13] B. Christianson: Reverse accumulation and attractive fixed points. Optimization Methods and Software, Taylor & Francis, 1994.

[14] M. Towara: A Discrete Adjoint Model for OpenFOAM. Procedia Computer Science, Elsevier, 2013.